Effect of Initial Total Monomer Concentration on the Swelling Behavior of Cationic Acrylamide-Based Hydrogels

John P. Baker,[†] Le H. Hong, Harvey W. Blanch, and John M. Prausnitz*

Department of Chemical Engineering, University of California, Berkeley, California 94720, and Chemical Sciences Division, Lawrence Berkeley Laboratory, 1 Cyclotron Road, Berkeley, California 94720

Received August 6, 1993; Revised Manuscript Received December 7, 1993[⊗]

ABSTRACT: The aqueous equilibrium swelling properties of a series of lightly-cross-linked cationic hydrogels based on acrylamide and [(methacrylamido)propyl]trimethylammonium chloride (MAPTAC) were measured as a function of initial total monomer concentration %*T* (w/v) and ionic strength. Swelling is a strong decreasing function of rising %*T*; the 10 %*T* hydrogel obtained a 17-fold larger swelling ratio (g of swollen hydrogel/g of dry hydrogel) in pure water compared to the 40 %*T* hydrogel. Good agreement is obtained between measured swelling equilibria in aqueous sodium chloride and that calculated from a Flory-type swelling model including ideal Donnan equilibria provided that an adjustable parameter is introduced into the swelling model for hydrogels in pure water. The experimental results presented here indicate that network-chain interpenetration increases with rising %*T*.

Introduction

Acrylamide-based hydrogels are synthesized on a regular basis in myriad biochemistry and molecular biology laboratories for the performance of polyacrylamide gel electrophoresis (PAGE).[1,2] In PAGE, biomacromolecules are fractionated based on their molecular weight and net charge. The desired effective median pore size of the polyacrylamide network is obtained by adjusting the weight ratio of total monomer to solvent and the mole fraction cross-linking monomer in the pregel reaction mixture. The pore sizes can be selected for optimal resolution between two macromolecular species. The wide range of applicability of PAGE is illustrated by the fractionation of oligonucleotides (MW < 1000) and high-molecular-weight RNA (MW > 10^6).[3]

A network prepared in solvent may have properties very different from those of a network prepared in bulk. A network prepared in solvent has a loose network structure, whereas a network prepared in bulk has a tight network structure resulting from interpenetration of polymer chains during network formation.

Acrylamide monomer is a solid at standard temperature and pressure (as is the homopolymer); the monomer must be dissolved in solvent for polymerization at these conditions. The amount of solvent (usually water) present at polymerization, or conversely the *initial total monomer concentration*, must be specified prior to the preparation of an acrylamide-based hydrogel because an acrylamide-based hydrogel may not be made in bulk. The initial total monomer concentration may be varied to alter the hydrogel structure and, in turn, alter the hydrogel properties. For this study, we define the initial total monomer concentration as the grams of monomer used for every 100 mL of solvent in the hydrogel feed solution; for brevity, we denote this parameter as "%*T*".

Several studies have been reported on the properties of hydrogels as a function of %*T*. These studies include swelling investigations,[4-10] analyses of microstructure via electron microscopy[11] and light scattering,[4] and investigations of mechanical properties.[4-7,9] In general, experimental observations are consistent with the concept of increasing chain interpretation with rising %*T*.

Hooper et al.[10] investigated the swelling properties of hydrogels prepared by copolymerizing acrylamide with the strong electrolyte [(methacrylamido)propyl]trimethylammonium chloride (MAPTAC). The authors systematically varied the hydrogel-composition parameters of mole percent charged comonomer, mole percent cross-linking monomer, and initial total monomer concentration (%*T*), and studied the effects of these parameters on swelling equilibria. The Flory–Rehner framework[12,13] for network swelling was used by Hooper et al.[10] to describe their experimental results. The effects of cross-link density and charge density on swelling equilibria were described reasonably well by the theory presented by Hooper et al., while the effect of %*T* on swelling was not reproduced correctly. Hooper et al. hypothesized that the inability of their swelling theory to describe the observed %*T* influence on swelling was related to the rise of (interchain) entanglements with increasing %*T* and to the absence in the theory of a strong contribution to network elasticity resulting from entanglements.

Our purpose of the present study is to measure swelling equilibria for a series of cationic poly(acrylamide-*co*-MAPTAC) hydrogels that are identical except for the %*T* of their pregel reaction mixtures. A second purpose is to improve Hooper et al.'s[10] poor description of acrylamide-based hydrogel swelling equilibria as a function of %*T*. As for Hooper et al., the Flory–Rehner theory provides the framework for our swelling description.

Experimental Section

Materials. Acrylamide and *N,N'*-methylenebis(acrylamide) (BIS) (both "electrophoresis grade") were purchased from Kodak. Ammonium persulfate (APS) and sodium chloride (NaCl) were purchased from Fisher. [(Methacrylamido)propyl]trimethylammonium chloride (MAPTAC) (50% solution in water) was purchased from Aldrich. All reagents were used as received. Water was distilled, then filtered and deionized with a Barnstead Nanopure II unit.

Synthesis. Acrylamide-based hydrogels with cationic character were prepared by the aqueous free-radical copolymerization of acrylamide, MAPTAC, and BIS, the cross-linking agent. APS was used to initiate the polymerization; the initiator concentration was held at a constant value of 0.5 mg/mL for all syntheses.

The nominal hydrogel composition is determined by the relative amounts of monomers and diluent (water) present in the

---

* To whom correspondence should be addressed.

[†] Present address: School of Pharmacy, Room S-926, University of California, San Francisco, CA 94143-0446.

[⊗] Abstract published in *Advance ACS Abstracts*, February 15, 1994.

0024-9297/94/2227-1446$04.50/0

pregel reaction solution. The following variables are convenient for defining this composition:

$$\%T = \frac{\text{mass of all monomers (g)}}{\text{volume of water (mL)}}100 \quad (1)$$

$$\%C = \frac{\text{mol of BIS in feed solution}}{\text{total mol of monomer in feed solution}}100 \quad (2)$$

$$\%MAPTAC = \frac{\text{mol of MAPTAC in feed solution}}{\text{total mol of monomer in feed solution}}100 \quad (3)$$

We use $\%T$ interchangeably with the phrase "initial total monomer concentration".

A series of hydrogels was prepared such that $\%C$ and $\%MAPTAC$ were fixed at 0.2% and 3%, respectively, while $\%T$ was varied; the $\%T$ values used were 10, 15, 20, 25, 30, 35, and 40. Continuous networks were not formed when $\%T$ was below 10. $\%T$ values greater than 40 were not considered for this study for two reasons: (1) At 25 °C, solutions with $\%T$ greater than 25 reach their gel points so quickly as to preclude injecting the hydrogel-feed solution into molds; the higher the $\%T$, the quicker the gel point is reached. To delay the gel point, all of the hydrogel-feed solutions were cooled in an ice bath for this work. (2) The influence of rising $\%T$ on the swelling properties of the resulting hydrogels diminishes as $\%T$ approaches 40.

To illustrate the synthetic procedure, we give details for the preparation of one hydrogel (30 $\%T$, 0.2 $\%C$, 3 $\%MAPTAC$). Added to 54.4 mL of gas-free water were 16.35 g of acrylamide, 0.073 g of BIS, and 3.15 mL of MAPTAC solution. An initiator solution was also prepared: 0.150 g of APS was dissolved in 20.0 mL of gas-free water. Both aqueous solutions were placed in an ice bath and stirred with magnetic spin bars until the monomers were completely dissolved (about 10 min). A 4.0-mL portion of the APS solution was added to the monomer solution; immediately after complete mixing, the monomer solution was injected (with a syringe fitted with a large-bore needle) between silanized glass plates separated by a 1.6-mm-thick Teflon spacer. The plates were immersed in a thermostated water bath at 50 °C. After 24 h, the hydrogel sheets were freed from the plates; disks were punched from the plates using a 10-mm-diameter cork borer. The hydrogel disks were soaked in water which was refreshed periodically to extract the soluble fraction and initiator residues. The soluble fraction for very similar poly(acrylamide-*co*-MAPTAC) hydrogels was measured by Baker et al.;[14] it is on the order of 0.1% of the dry mass.

Swelling Studies. After synthesis, the hydrogel disks were placed in pure water where they were allowed to swell to equilibrium. To monitor the swelling of the hydrogels, the masses of the hydrogels were measured periodically. Approximately 1 week was required to reach equilibrium swelling in water. Once equilibrium was attained, the hydrogels were weighed, dried at room temperature and atmospheric pressure, and then reweighed. The swelling ratio in water is defined as the mass ratio of swollen hydrogel to dry hydrogel.

Similar procedures were performed for swelling studies in aqueous NaCl. The ionic strength of the salt solutions ranged from 10^{-5} to 1.0 M. Water-equilibrated hydrogel disks were placed in aqueous NaCl solutions and allowed to swell to equilibrium; approximately 10 days were needed to reach equilibrium. The approach to equilibrium of the hydrogels was monitored gravimetrically. The swelling ratio of the hydrogels in the salt solutions in normalized by the swelling ratio in water:

$$\text{Swelling ratio in NaCl}_{(aq)} = \left(\frac{\text{mass gel in salt solution}}{\text{mass gel in water}}\right)\left(\frac{\text{mass gel in water}}{\text{mass dry gel}}\right) \quad (4)$$

Each swelling ratio reported in this paper is an average of two separate swelling measurements performed in parallel.

Elemental Microanalysis. Elemental microanalyses (U. C. Berkeley College of Chemistry Microanalytical Laboratory) were performed on dried, pulverized hydrogel samples that had been extracted in water.

Compressive Stress–Strain Measurements. Compressive stress–strain experiments were performed on all hydrogels prepared except the one prepared with 10 $\%T$; this hydrogel was too compliant for the experimental treatment. Hydrogel disks, equilibrium-swollen in water, were compressed to 5% strain in steps of 0.25% strain by a Rheometrics Solids Analyzer II apparatus. The aspect ratio (length/diameter) for all hydrogels tested was held constant at 0.29. Measurements were made for two samples for each hydrogel lot. The results were averaged.

Measurement of Sodium Partition Coefficients. Sodium partition coefficients were measured for all hydrogels prepared for this study for the purpose of estimating their fixed-charge densities. For these measurements, 100-mL beakers were charged with 25 mL of 10^{-3} M NaCl solution and 25 mL of water-equilibrated hydrogel. The beakers were sealed for 10 days to allow for equilibration. The masses of the hydrogels and external solutions were measured. The sodium concentrations of the external solutions were measured using a Perkin-Elmer Model 2280 atomic absorption spectrophotometer. Sodium concentrations inside the hydrogels were determined from mass balances. The sodium partition coefficient is defined as the concentration of sodium in the external solution divided by that in the hydrogel. Duplicate partition experiments were performed for each $\%T$. The results were averaged.

Swelling Theory for Hydrogels

The framework which defines swelling equilibria in gel/solvent systems has existed for many years;[12,15] it is a direct extension of the basis for defining phase equilibria in linear-chain polymer solutions. For equilibrium between two coexisting phases α and β, the chemical potential μ of every component i is the same in both phases, i.e.

$$\mu_i^{\alpha} = \mu_i^{\beta} \quad (5)$$

For swelling of a hydrogel in a solvent, α represents the gel phase and β represents the external phase, or bath surrounding the gel. Equation 5 applies for all components which can exist in both phases, i.e., for all diffusible species. When i represents the solvent (component 1), eq 5 is commonly recast in the form

$$\Delta\Pi_{\text{swelling}} = -\frac{\mu_1^{\text{gel}} - \mu_1^{\text{bath}}}{V_1} = 0 \quad (6)$$

where $\Delta\Pi_{\text{swelling}}$ is the osmotic swelling pressure and V_1 is the solvent molar volume. When nonzero, $\Delta\Pi_{\text{swelling}}$ provides a driving force for hydrogel volume change.

$\Delta\Pi_{\text{swelling}}$ shows a complex dependence on hydrogel and solution properties. The commonly-used Flory–Rehner theory[13] consists of three contributions

$$\Delta\Pi_{\text{swelling}} = \Delta\Pi_{\text{mixing}} + \Delta\Pi_{\text{elastic}} + \Delta\Pi_{\text{ion}} = 0 \quad (7)$$

where $\Delta\Pi_{\text{mixing}}$ is the contribution from polymer/solvent mixing, $\Delta\Pi_{\text{elastic}}$ is the elastic contribution from deforming the network chains from their reference state, and $\Delta\Pi_{\text{ion}}$ represents the contribution from ion/solvent mixing and electrostatic effects. Equation 7 is analogous to a mechanical equilibrium balance—solvent moves into or out of the hydrogel until $\Delta\Pi_{\text{swelling}}$ is zero, i.e., until the three forces working to expand or contract the hydrogel are balanced. Equation 7 coupled with eq 5 defines the degree of swelling (equilibrium gel composition) for specified conditions.

The Flory–Rehner theory contains several assumptions that have been the subject of much discussion. The first assumption is the principle of separability of the elastic and polymer/solvent mixing contributions to the total swelling pressure.[16-24] The second assumption is that $\Delta\Pi_{\text{mixing}}$ is given by the theoretical description of polymer/

solvent mixing for the un-cross-linked, infinite-molecular-weight polymer solution at the same concentration and in the same solvent as those of the network.[4,25-29]

An examination of the validity of the assumptions inherent in the Flory–Rehner theory is beyond the scope of the present study. We accept the first assumption that the elastic, mixing and ion terms are linearly additive. However, we recognize that assuming that the $\Delta\Pi_{\mathrm{ion}}$ term is separable is questionable because placing hydrophilic fixed-charge groups onto a polymer should have an influence on polymer/solvent mixing. For our purposes here, we assume that the fraction of charged structural units in the networks prepared for this study is sufficiently low to have a negligible effect on the $\Delta\Pi_{\mathrm{mixing}}$ term. This assumption appears to be valid for highly-swollen, lightly-charged hydrogel networks.[10,30] We are not concerned here with the second assumption, because for $\Delta\Pi_{\mathrm{mixing}}$ we use the Flory–Huggins theory[13] with a Flory χ parameter fitted to network swelling data.

To use eq 7, we must specify the dependence of the three swelling-pressure contributions on hydrogel and solution properties. As stated above, we use Flory–Huggins theory for $\Delta\Pi_{\mathrm{mixing}}$

$$\Delta\Pi_{\mathrm{mixing}} = -\frac{RT}{V_1}(\ln(1-\phi_2) + \phi_2 + \chi\phi_2^{\,2}) \qquad (8)$$

Here, R is the gas constant, T is temperature, ϕ_2 is the volume fraction of polymer in the hydrogel, V_1 is the molar volume of the solvent, and χ is the Flory parameter that characterizes the polymer–solvent interaction energy.

Because of complex polymer/solvent mixing effects, the applicability of eq 8 to hydrogel systems is questionable. More realistic models for polymer/solvent mixing in aqueous systems are available.[31,32] However, these models are more complex mathematically than the Flory–Huggins theory. For highly-swollen polyelectrolyte hydrogels, it has been noted that $\Delta\Pi_{\mathrm{mixing}}$ is usually small compared to $\Delta\Pi_{\mathrm{ion}}$ and $\Delta\Pi_{\mathrm{elastic}}$.[33,34] An order-of-magnitude analysis of the terms in eq 7 shows that the influence of χ becomes minor for charged hydrogels at high degrees of swelling. Therefore, we take a simple approach and use the Flory–Huggins equation for $\Delta\Pi_{\mathrm{mixing}}$.

To obtain a reasonable value for χ, we regressed the Flory χ parameter from swelling data reported by Hooper et al.[10] for uncharged acrylamide-based hydrogels equilibrium swollen in pure water. For the regression (within the Flory–Rehner approximation), eq 8 was used for $\Delta\Pi_{\mathrm{mixing}}$ and eq 9 was used for $\Delta\Pi_{\mathrm{elastic}}$ (N set equal to unity); $\Delta\Pi_{\mathrm{ion}}$ was set equal to zero. A best-fit value for χ of 0.48 was obtained; χ was held constant at this value in the calculations described here.

The two most common network-elasticity theories consider the idealized cases of the affine network[13] and the phantom network.[35] These two theories can be considered to be the two limits of a continuum of descriptions of how neighboring chains (constraints) effect cross-link fluctuations (Brownian motion). In the affine network, cross-link fluctuations are totally suppressed and components of each chain vector transform linearly with deformation. In the phantom network, cross-links fluctuate freely, unaffected by the presence of neighboring chains or by the state or deformation. The affine network model is frequently used to describe the elastic contribution to gel swelling. However, this model gives a poor description of elastic properties when applied over a large range of strain, and is particularly unsuitable for swollen networks whose properties are presumably closer to those of a phantom network.[36] For isotropic swelling of a perfect tetrafunctional network, elasticity theory gives:

$$\Delta\Pi_{\mathrm{elastic}}^{\mathrm{phantom}} = -C_c RTN\left(\frac{\phi_2}{\phi_{2c}}\right)^{1/3} \qquad (9)$$

$$\Delta\Pi_{\mathrm{elastic}}^{\mathrm{affine}} = -2C_c RT\left[\left(\frac{\phi_2}{\phi_{2c}}\right)^{1/3} - \frac{1}{2}\left(\frac{\phi_2}{\phi_{2c}}\right)\right] \qquad (10)$$

where C_c is the concentration of crosslinks in the reference state, i.e. at hydrogel preparation, ϕ_{2c} is the volume fraction of hydrogel in the reference state, and N is an empirical parameter. For highly swollen networks, the second term of the affine theory (the so-called volume term[37]) is small; thus, the limiting theories differ by a factor of 2. N can be regressed from swelling data to give an estimate of the effective cross-link density for a hydrogel. Equations 9 and 10 are derived elsewhere.[36,38]

Fixed charges on the network are confined to the hydrogel phase, along with an equal number of counterions. Because of the fixed charges, there is an unequal distribution of mobile ions between the hydrogel and the external solution, producing an osmotic-pressure difference between the two phases. This osmotic-pressure difference introduces an additional contribution to the swelling pressure. Ideal Donnan equilibria have been used successfully to characterize this contribution to the swelling pressure for acrylamide-based hydrogels.[10,30] A complete description of the effect of fixed and mobile ions on hydrogel swelling would require expressions for ion–ion, ion–solvent, and ion–polymer interactions; these interactions are neglected in the ideal Donnan equilibria, giving the expression

$$\Delta\Pi_{\mathrm{ion}} = RT\sum_i (C_i^{\mathrm{gel}} - C_i^{\mathrm{bath}}) \qquad (11)$$

where C_i^{gel} and C_i^{bath} represent, respectively, mobile ion concentrations within the hydrogel and in the bath surrounding the hydrogel. Equation 11 assumes that the ion concentrations are small and the osmotic coefficient is unity.[39]

The concentration of ions in the external solution is fixed by experimental conditions. The concentration of mobile ions within the hydrogel is calculated (for use in eq 11) according to ideal Donnan equilibria: the chemical potential of an ionic species in the hydrogel phase must be equal to its chemical potential in the external solution, and the constraint of electroneutrality is placed on all charged species, fixed and mobile, in the hydrogel phase. For a hydrogel in solution containing a single 1:1 salt we have

$$(C_+^{\mathrm{gel}})(C_-^{\mathrm{gel}}) = (C_s^{\mathrm{bath}})^2 \qquad (12)$$

where C_s^{bath} refers to the concentration of 1:1 electrolyte in the external solution. Equation 12 assumes that the mean ionic activity coefficient of the diffusible salt in the hydrogel phase is equal to that in the bath. To maintain electroneutrality, the number of positive ions must equal the number of negative ions in the hydrogel phase. We write for univalent electrolytes

$$C_+^{\mathrm{gel}} + I\,C_{\mathrm{mc}}\frac{\phi_2}{\phi_{2c}} = C_-^{\mathrm{gel}} \qquad (13)$$

where I represents the fraction of structural units in the hydrogel that contain bound positive charges and C_{mc} denotes the molar concentration of monomer at network formation. The second term on the left-hand side of eq

13 gives the concentration of fixed positive charges in the hydrogel phase.

Equilibrium swelling for a given hydrogel and solution conditions is determined by substituting eqs 8, 9 (or 10), and 11 into eq 7 and substituting for C_+^{gel} in eq 12 by using eq 13. These steps leave two equations with two unknowns, ϕ_2 and C_-^{gel}. An iterative procedure using a generalized Newton–Raphson routine was used to solve the equations.

Theory for Networks in Uniaxial Compression (or Extension)

We assume that the sample volume and composition remain constant with deformation. For both the phantom and affine network theories, the axial force f acting along the x axis for a network in compression is[36]

$$f = 2\left(\frac{F\,k\,T}{L_{i1}}\right)\left(\frac{V}{V_c}\right)^{2/3}(\alpha - \alpha^{-2}) \qquad (14)$$

where k is the Boltzmann constant, V is the volume of the undistorted, swollen network, V_c is the volume of the network at preparation, L_{i1} is the initial, undistorted, axial length of the network at volume V, α is the deformation ratio relative to the initial sample dimensions, and F is the elastic "front factor". For a perfect, tetrafunctional network F equals $\nu/2$ for the affine model and $\nu/4$ for the phantom model, where ν is the number of chains in the network. Equation 14 is derived from first principles elsewhere.[13,36,38]

For comparison with theory, experimental data are generally represented in terms of the reduced stress $[f^*]$:

$$[f^*] = \frac{f\phi_2^{1/3}}{A_d(\alpha - \alpha^{-2})} \qquad (15)$$

where A_d is the cross-sectional area of the undeformed, dry sample (subscript d denotes the dry sample). We note the following relations before proceeding:

$$\phi_2^{1/3} = L_d/L_{i1} \qquad (16)$$

$$V_d = A_d\,L_d \qquad (17)$$

$$\phi_{2c} = V_d/V_c \qquad (18)$$

Inserting eq 15 into eq 14 leads to

$$[f^*] = 2\left(\frac{F\,k\,T}{V_d}\right)\phi_{2c}^{2/3} \qquad (19)$$

Noting that, for a perfect tetrafunctional network, the number of cross-links C equals $\nu/2$ and using eq 18, we obtain

$$[f^*]_{\text{phantom}} = C_c R T \phi_{2c}^{-1/3} \qquad (20)$$

$$[f^*]_{\text{affine}} = 2C_c R T \phi_{2c}^{-1/3} \qquad (21)$$

Equations 20 and 21 show that for a phantom network or an affine network, the reduced stress is predicted to be independent of deformation and swelling. However, ample experimental data show that $[f^*]$ does depend on deformation and swelling.[40–43]

Charge Density Estimation via Donnan Exclusion

When a hydrogel with a net positive-charge density is in equilibrium with a 1:1 electrolyte (aqueous) solution, the mobile cations are partially excluded from the hydrogel via Donnan exclusion.[44,45] Information of ion partitioning between hydrogel and external solution may be used to estimate the charge density of an ionized hydrogel.[34] The equations for Donnan equilibria presented above may be used to estimate hydrogel charge densities. Equation 13 may be substituted into eq 12 to eliminate C_-^{gel}, resulting in the following equation (for 1:1 electrolytes):

Table 1. Elemental Microanalytical Results for %T-Varying Poly(acrylamide-*co*-MAPTAC) Hydrogels[a]

element	observed	theoretical
C	42.0(0.1)	42.0
N	15.3(0.1)	16.0
H	7.81(0.05)	8.0

[a] The observed results are presented as an average over all seven gels prepared; values in parentheses are standard deviations. Theoretical values are calculated assuming 5 wt % water was trapped inside the collapsed, dry networks submitted for analysis.

$$(C_+^{gel})\left(C_+^{gel} + I\,C_{mc}\frac{\phi_2}{\phi_{2c}}\right) = (C_+^{bath})^2 \qquad (22)$$

I, the fraction of hydrogel structural units containing fixed-positive charges, may be calculated using eq 22 provided the following quantities are known: C_{mc}, the molar concentration of monomer at network formation; ϕ_{2c}, the volume fraction of polymer in the hydrogel at preparation; and C_+^{bath}/C_+^{gel}, the partition coefficient of the diffusible cation between the external solution (bath) and hydrogel.

Results and Discussion

Since only the initial total monomer concentration %T differed between all hydrogels synthesized, all hydrogels should have the same elemental composition. Table 1 shows the results from elemental microanalysis. Excellent agreement between samples was observed. The favorable microanalysis allows us to use %T as a basis for comparing the hydrogels in this study.

Interpretation of the elemental-microanalysis data is complicated by the chemical similarity of the monomers. We could not invert the microanalysis data to give monomer mole fractions. Interpretation of the data is further complicated by the presence of residual solvent (water) in the dried hydrogel samples submitted for analysis. Since hydrogels are composed of hydrophilic polymer, some water is adsorbed to the polymer backbone. Water is inevitably trapped in the interior as a preswollen hydrogel particle dries.

The theoretical weight percents of atomic elements for a copolymer hydrogel may be computed from the known composition of the original monomer solution, assuming complete monomer conversion. Also shown in Table 1 are theoretical estimates of the elemental composition based on the reaction stoichiometry. When making the calculations we assumed the samples submitted for analysis contained 5% adsorbed/trapped water. The calculated values agree qualitatively with the observed values.

Figure 1 shows measured swelling equilibria in deionized water for poly(acrylamide-*co*-MAPTAC) hydrogels as a function of the initial total monomer concentration %T. The cross-link density was fixed at 0.2 %C and the charge density was fixed at 3.0 %*MAPTAC* for these hydrogels. As expected, swelling in water declines with rising %T. Also shown in Figure 1 are predicted swelling curves calculated using the swelling model presented above; the predicted curves for the phantom model and the affine model were generated by using eq 9 and eq 10 in the calculations, respectively. The nominal hydrogel composition parameters (%T, %C, and %*MAPTAC*) were used in the calculations. The observed dependence of

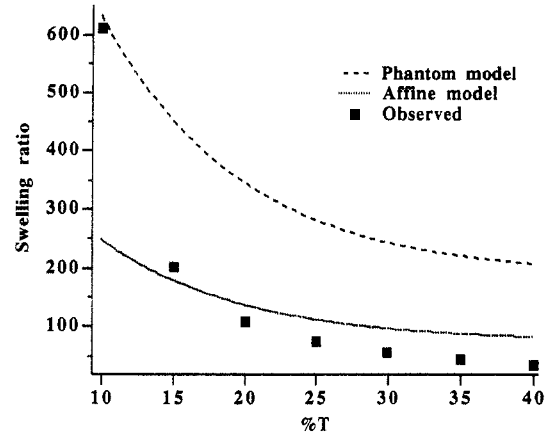

Figure 1. Swelling ratios (g of swollen gel/ g of dry gel) in water for poly(acrylamide-*co*-MAPTAC) hydrogels prepared with varying initial total monomer concentrations % *T*. The observed swelling ratios are compared with model predictions. Predicted swelling curves were generated using the nominal values of the hydrogel structural parameters (% *T*, 0.2 % *C*, 3.0 % *MAPTAC*).

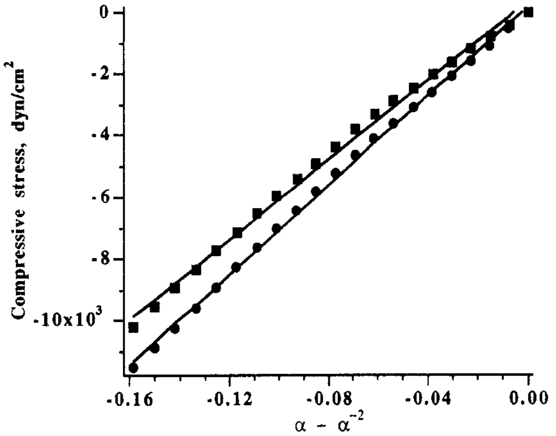

Figure 2. Compressive stress–strain data for the 25 % *T* hydrogel samples. The hydrogel was equilibrium-swollen in pure water before the compressive tests were performed.

swelling on % *T* is stronger than those predicted by the affine and phantom models; this result is similar to that reported by Hooper et al.[10]

Use of the nominal values of the cross-link density and charge density of the hydrogels in the swelling calculations leads to poor agreement between theory and experiment (see Figure 1). We therefore obtained, from independent experiments, effective values for these parameters. The cross-link densities of the hydrogels were estimated by conducting mechanical stress–strain analyses, while the charge contents of the hydrogels were estimated from the Donnan exclusion of sodium ions.

% *T*-varying hydrogel disks, equilibrium swollen in pure water, were subjected to compressive stress–strain analysis. Figure 2 shows representative compressive stress–strain data for the two runs performed on the 25 % *T* hydrogel samples; as predicted by theory, reasonably straight lines are obtained when the stress (force per unit sample area) is plotted against the quantity ($\alpha - \alpha^{-2}$). For the 15, 20, 30, 35, and 40 % *T* hydrogels, stress–strain data were of similar quality.

Compression moduli for the 25 % *T* samples were obtained from the slopes of best-fit lines drawn through the data in Figure 2. Table 2 and Figure 3 shows compression moduli for all hydrogels analyzed. An interesting aspect of Figure 3 is that a best-fit line through the moduli does not intersect with the origin, but intersects with the positive abscissa at roughly 11 % *T*. This occurs because at high diluent concentrations (low % *T* values), cross-links tend to be wasted in network defects such as elastically ineffective loops and unreacted pendant double bonds.[7,36,46] The growing chains are so dilute that some cross-links are wasted as chains cross-link upon themselves, forming loops. Pendant double bonds tend to have lower relative reactivities because of steric hindrance. The probability that a pendant double bond is met by an active radical site during synthesis is lowered at high diluent concentrations; some pendant double bonds may not react at all. Therefore, for acrylamide-based systems at low % *T* values, the effective cross-link density is probably less than the nominal cross-link density. As % *T* rises, it is likely that the efficiency of cross-linking improves. At % *T* values below 10 (with a % *C* of 0.2 and a % *MAPTAC* of 3), cross-link wastage is so prevalent that no continuous network is formed. We were able to produce a hydrogel using 10 % *T* but, as the intercept of the plot predicts, this hydrogel was too fragile to be subjected to mechanical testing. Results similar to those shown in Figure 3 were obtained by Oppermann et al.[7] for un-ionized polyacrylamide hydrogels tested in the unswollen state.

Table 2. Swelling Ratios and Compressive Stress–Strain Moduli for % *T*-Varying Poly(acrylamide-*co*-MAPTAC) Hydrogels in Fresh Water[a]

% *T*	swelling ratio, g of swollen gel/g of dry gel	Modulus × 10^4, dyn/cm^2	*N*
10	613.0(5.0)		1.02
15	200.9(2.0)	2.7(0.2)	1.70
20	106.9(1.7)	6.1(1.1)	2.22
25	75.5(1.4)	6.8(0.5)	2.49
30	55.4(0.1)	10.1(0.5)	2.81
35	44.5(0.1)	12.8(3.6)	3.04
40	36.2(1.4)	18.7(0.6)	3.30

[a] The hydrogels were prepared with 0.2 % *C* and 3 % *MAPTAC*. Values in parentheses are standard deviations. Also listed are values for the empirical parameter *N*; see the text for an explanation of *N*.

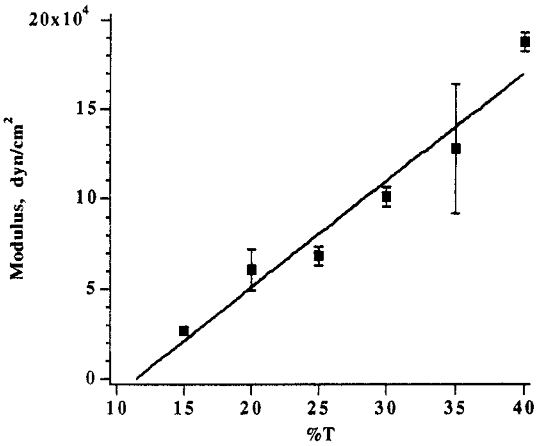

Figure 3. Compression moduli determined from compressive stress–strain measurements for hydrogels prepared with different % *T*.

In Figure 4, we compare predictions of the phantom model limit and affine model limit (eqs 20 and 21, respectively) to experimental compressive stress–strain data for poly(acrylamide-*co*-MAPTAC) hydrogel networks prepared with different % *T*. The observed [f^*], calculated using eq 15, are in fair agreement with those predicted by the phantom model. This agreement is reasonable because at high degrees of swelling, the effect of constraints on cross-link fluctuations diminish; the phantom theory assumes that constraints have no effect on network elasticity. Stress–strain behavior coinciding with the phantom limit has been observed in compression and in tension for swollen networks ($\phi_2 \geq 0.2$).[42] (We are

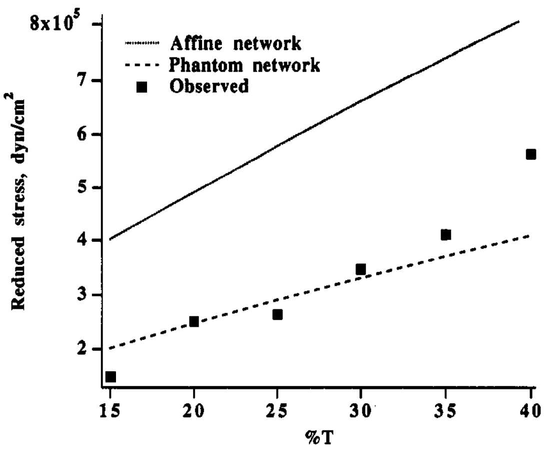

Figure 4. Reduced stress $[f^*]$ plotted as a function of % *T*. Here experiment is compared with predictions from the phantom and affine theories of elasticity.

considering *highly* swollen networks in the present work; ϕ_2 was about 0.03 for the 40 % *T* hydrogel equilibrium swollen in water and about 0.005 for the 15 % *T* hydrogel.) A negative deviation from the phantom theory is observed for the 15 % *T* hydrogel, consistent with the idea of a significant fraction of wasted cross-links for this hydrogel. A positive deviation from phantom theory is seen with the 40 % *T* hydrogel, consistent with the concept of rising entanglement density with increasing % *T*.[5,6] Interchain trapped entanglements add to the mechanical strength of a network material by acting as effective cross-links.[47,48]

The results shown in Figure 4 indicate that the phantom theory of elasticity adequately describes the compressive stress–strain behavior in water for highly-swollen poly(acrylamide-*co*-MAPTAC) hydrogels. It appears that network defects (loops, entanglements, unreacted pendant double bonds) play a minor role in the stress–strain behavior of the hydrogels studied here. The results shown in Figure 4 are clearly inconsistent with the results for swelling equilibria shown in Figure 1. Other authors have reported similar results for hydrophilic networks.[34,49] The inconsistency may to be related to differences in the elastic response of chain entanglements and other physical interactions (e.g., hydrogen bonding) caused by isotropic swelling or compressive mechanical deformation.[17,34]

The theory upon which the phantom model is based assumes that the network chains obey Gaussian statistics.[36,38] Gaussian statistics allows for network chains to be extended to infinity; however, real chains have finite extendibility.[38,50] Although the results shown in Figure 4 are for highly-swollen hydrogels (consisting of at least 98% water), non-Gaussian corrections[51,52] to the phantom elasticity theory (to correct for the finite extendibility of the network chains) appear not to be needed.

The fair agreement between theory and experiment seen in Figure 4 may be the result of a fortuitous compensation: low effective cross-linking density is compensated by finite extendibility of network chains. In light of this possibility, the hydrogels in this study should be considered as "effective" phantom networks with effective cross-link densities coincidentally close to the nominal values.

Donnan-exclusion measurements of sodium ions from the positively-ionized, % *T*-varying hydrogels were conducted for the purpose of estimating hydrogel charge densities. Table 3 lists and Figure 5 shows sodium partition coefficients (external sodium concentration/hydrogel sodium concentration) obtained from the procedure described earlier. As expected, sodium exclusion is an increasing function of % *T*. The concentration of fixed charges in the hydrogels based on polymer (% *MAPTAC*) is nominally constant for the hydrogels in this study; however, the concentration of fixed charges based on *hydrogel volume* rises with increasing % *T*. The higher the fixed-charge concentration based on hydrogel volume, the more efficient is the hydrogel in excluding sodium.

Table 3. Sodium Partition Coefficients Obtained from the Donnan-Exclusion Experiment Described in the Text[a]

%T	partition coefficient[b]	I^c	%T	partition coefficient[b]	I^c
10	2.8(1.1)	2.2	30	8.4(0.6)	1.6
15	3.9(0.4)	2.1	35	14.7(8.3)	2.4
20	4.2(0.2)	1.2	40	16.6(2.7)	2.2
25	6.2(0.4)	1.4			

[a] Also listed are values for the hydrogel fixed-charge density *I* calculated using eq 21. The nominal value for *I* is 3%. [b] (Concentration sodium in external solution)/(concentration of sodium in the hydrogel). [c] Expressed as the percent positively-ionized structural units in the hydrogels

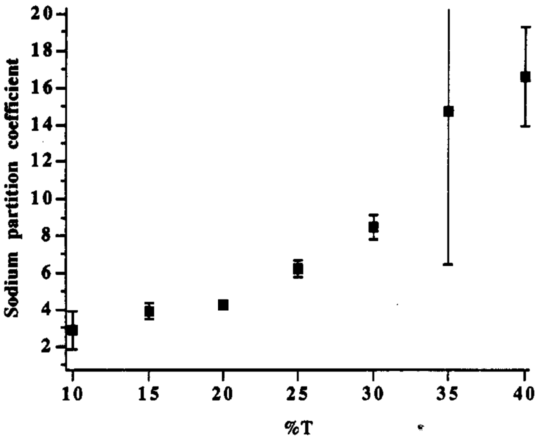

Figure 5. Sodium partition coefficients determined from % *T*-varying hydrogels. The partition experiment is described in the text.

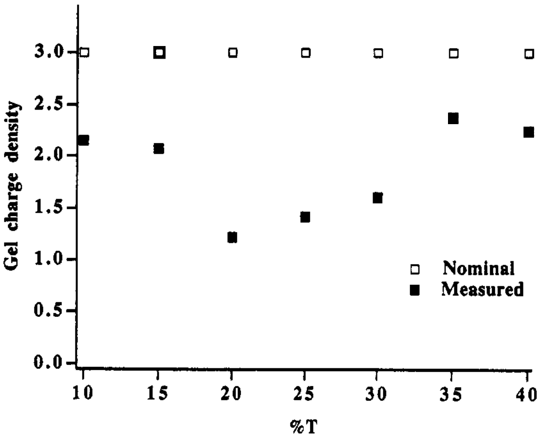

Figure 6. Effective hydrogel charge densities determined for % *T*-varying hydrogels. The effective charge densities were estimated from the ideal Donnan partitioning of sodium ions into the hydrogels. The hydrogels were nominally prepared with 3% cationic monomer.

Effective values of *I*, the fraction of cationic structural units in the hydrogels, were calculated from eq 22 using the results of the partition experiments. Table 3 lists and Figure 6 shows *I* (expressed as a percentage) as a function of % *T*. The nominal value of *I* is 3.0%, while the measured value is 1.9% (averaged across all % *T*). Apparently 37% of the fixed cationic charges are "missing". Two mechanisms, possibly working in concert, may explain the missing the charge density. It is possible that a fraction of cationic functionalities are missing from the hydrogel networks: some positively-ionized MAPTAC monomers may not have been incorporated into the network during synthesis; some fixed-cationic functionalities may have been removed after synthesis via amide hydrolysis. More likely, given the majority of acrylamide-derived structural units in the hydrogels, hydrolysis of pendant amide functional groups to anionic carboxylate groups is responsible for masking some of the cationic charges.

The base-catalyzed hydrolysis of polyacrylamide to give carboxylate functionalities in the polymer chain is a well-known reaction.[53-57] Conditions favorable for amide hydrolysis existed for the hydrogels in this study during synthesis.[53] Although slow under mild conditions, rates of polyacrylamide hydrolysis are known to increase with rising temperature: the hydrogels were synthesized at 50 °C for 24 h. Also, the cationic character of the poly(acrylamide-*co*-MAPTAC) network chains provide for the local enhancement of the concentration of OH^- ions via electrostatic attraction.

The elemental microanalysis results provide independent evidence for hydrolysis of pendant amide groups to carboxylate functionalities. Ammonia is the product of base-catalyzed amide hydrolysis.[58] A comparison of calculated and observed results shows that the hydrogel nitrogen and hydrogen contents are lower than expected from the reaction stoichiometry. From the microanalytical results, we estimate amide hydrolysis to be on the order of a few percent for the hydrogels in this study. Significant loss of elemental nitrogen from the hydrogels via hydrolysis of cationic MAPTAC structural units to anionic methacrylate structural units would involve a concomitant loss of elemental carbon from the hydrogels. Loss of elemental carbon via hydrolysis of MAPTAC units is not supported by the microanalytical results. In other words, the elemental carbon to nitrogen ratio increases upon acrylamide-unit hydrolysis and decreases upon MAPTAC-unit hydrolysis; the observed carbon to nitrogen ratio supports acrylamide-unit hydrolysis.

For positively ionized hydrogels equilibrium swollen in low-ionic-strength media, the pH in the hydrogen interior is likely much higher than neutral because of Donnan exclusion of protons. Therefore, since the nominal pK_a of acrylic acid is 4.3, any hydrolysis products on the network chains will be fully ionized to the carboxylate form.

The fixed-charge density of a hydrogel is measured indirectly from a Donnan-exclusion experiment. The actual number of fixed charges is not determined—only the net charge is determined. For example, an exclusion experiment based on ideal Donnan equilibria will necessarily give the same answer if the hydrogel contains a cationic fixed-charge density of 2 mol % and an anionic fixed-charge density of zero or a cationic fixed-charge density of 3 mol % and an anionic fixed density of 1 mol %. For highly-swollen lightly-charged hydrogels, it is known that swelling is governed by the net charge of the hydrogel.[59,60] The net charge is important because it is the osmotically-active counterions that principally drive the swelling of highly-swollen lightly-charged hydrogels. In pure water, hydrogels containing both cationic fixed charges and anionic fixed charges (ampholytic hydrogels) may become self-neutralized to a degree; excess free ions not needed to satisfy electroneutrality are dialyzed from the hydrogel interior. If some hydrolysis has occurred, then the hydrogels in this study are partially self-neutralized and the concentration of osmotically-active counterions inside the hydrogels is less than it would be with no hydrolysis.

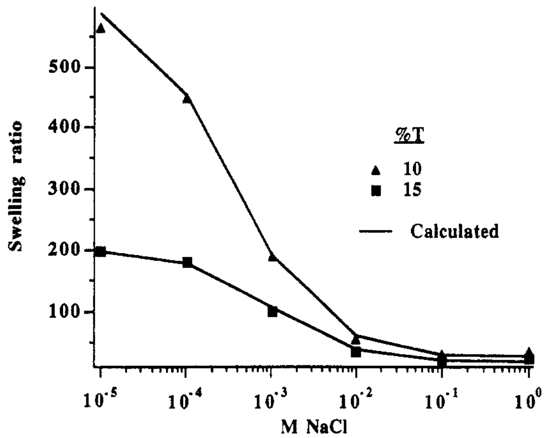

Figure 7. Swelling ratios (g of swollen gel/g of dry gel) in aqueous NaCl for poly(acrylamide-*co*-MAPTAC) hydrogels prepared with % *T* of 10 or 15: comparison of experiment with theory. The calculated points were generated at discrete NaCl concentrations; straight lines join the points to help guide the eyes.

Ilavsky et al.[57] prepared polyacrylamide solutions and hydrogels under similar conditions (favorable for hydrolysis) and measured the extent of amide hydrolysis during synthesis and aging of un-cross-linked polyacrylamide to infer the extent of amide hydrolysis during synthesis and aging in the corresponding hydrogel. Ilavsky et al.'s technique, the colorimetric detection of liberated ammonia, is not suitable for three-dimensional networks (hydrogels) because of mass transfer limitations.

Unfortunately, the lowered values of *I* for the hydrogels determined by the Donnan-exclusion experiments (Figure 6) only partially account for why the measured swelling equilibria in water shown in Figure 1 is overpredicted by the swelling theory. When the independently-obtained values for the charge density *I* (calculated from the Donnan exclusion experiments using eq 22) and cross-link concentration C_c (calculated from the compressive stress–strain data using eq 20) are inserted into the swelling theory (eq 7), quantitative agreement is not obtained between the observed swelling ratios and those predicted by theory.

To correct for deficiencies in our swelling description, we add the parameter *N* to the phantom theory (eq 9). We have used the swelling data shown in Figure 1 to fit values for *N* from eq 7; as expected, *N* is of order unity. Table 2 shows the fitted values of *N* for each corresponding % *T* value. *N* values range from 1.02 at 10 % *T* to 3.30 at 40 % *T*. We used the nominal hydrogel composition parameters (% *T*, 0.2 % *C*, 3.0 % *MAPTAC*) in the fits.

The fitted values of *N*, determined from swelling equilibria for the % *T*-varying hydrogels in water, are used to predict hydrogel-swelling equilibria in aqueous NaCl. Figure 7 shows measured and calculated swelling equilibria in aqueous NaCl solutions for hydrogels prepared with 10 or 15 % *T*; Figure 8 shows measured and calculated results for hydrogels with 20–40 % *T*. Calculated curves were generated by using eq 7 with fitted values for *N*. Agreement is good between measured and calculated results probably because the deficiencies of the theory are compensated by the parameter *N*, which is a function of % *T*.

Fitting the parameter *N* in the swelling model to swelling data in pure water is equivalent to fitting the *Y*-intercepts in Figures 7 and 8. We have fit the *Y*-intercepts in Figures 7 and 8 and then allowed the volume (ϕ_2) dependence of the swelling model to predict the shape of the swelling curve as a function of NaCl concentration. It appears that the volume dependence of the swelling model is correct; however, to obtain quantitative performance, the

Table 4. Swelling Ratios (g of swollen gel/g of dry gel) for % *T*-Varying Poly(acrylamide-*co*-MAPTAC) Hydrogels in Aqueous NaCl Solutions[a]

NaCl, m	10 % *T*	15 % *T*	20 % *T*	25 % *T*	30 % *T*	35 % *T*	40 % *T*
1.0×10^{-5}	565.2(21.2)	198.2(1.6)	107.9(3.7)	73.4(2.8)	54.5(0.1)	44.1(0.2)	35.5(1.1)
1.0×10^{-4}	446.3(20.7)	179.0(1.9)	98.1(5.5)	73.7(2.5)	53.9(0.3)	42.8(0.1)	35.0(1.3)
1.0×10^{-3}	187.9(9.7)	98.1(0.6)	63.8(1.2)	50.1(1.6)	40.4(0.3)	34.3(0.1)	29.2(0.8)
0.010	55.2(0.5)	34.4(0.4)	25.4(0.4)	22.3(0.1)	19.6(0.6)	17.5(0.2)	15.7(0.8)
0.10	29.6(0.3)	19.3(0.3)	15.0(0.7)	13.2(0.2)	11.9(0.4)	10.9(0.1)	9.9(0.1)
1.0	34.3(2.3)	22.6(0.1)	16.6(0.2)	14.6(0.1)	13.1(0.4)	12.2(0.1)	10.6(0.5)
5.0	43.9(1.4)	29.1(0.3)	21.6(0.7)	19.5(0.7)	17.1(0.6)	15.4(0.2)	13.8(0.4)

[a] Values in parentheses are standard deviations.

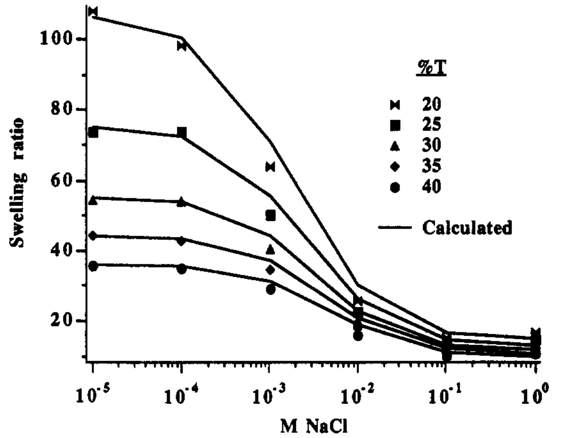

Figure 8. Swelling ratios (g of swollen gel/g of dry gel) in aqueous NaCl for poly(acrylamide-*co*-MAPTAC) hydrogels prepared with 20–40 % *T*: comparison of experiment with theory. The calculated points were generated at discrete NaCl concentrations; straight lines join the points to help guide the eyes.

model must be scaled to experimental data. The parameter *N* provides such scaling.

We insert a fitting parameter into the phantom elastic term (eq 9) to correct for deficiencies in the swelling theory to obtain agreement between measured and calculated swelling equilibria. Our adjustable parameter is equivalent to fitting an effective cross-link density to experimental data. Others,[52,57,61,62] studying acrylamide-based hydrogels containing weakly-ionizable acid groups, introduce the osmotic coefficient into the ion term of the swelling theory (eq 12) and adjust this coefficient to obtain agreement between measured and calculated swelling equilibria. This alternative may be viewed as assuming an effective degree of ionization for the fixed-charge groups. We have used the cell model for polyelectrolytes,[39,63] supplemented by the additivity rule, to estimate osmotic coefficients. Our calculations show that this coefficient is never less than 0.96 for the conditions found in the present study. The very small deviation from ideality (unity) is due to the low charge density of the network chains. Therefore, as a simplifying assumption, we have set the osmotic coefficient equal to unity in our calculations.

In our swelling model, we have assumed that the mean ionic activity coefficient of the the diffusible salt in the hydrogel phase is equal to that in the bath. The Debye–Hückel theory of electrolyte solutions[64] (valid for ionic strengths of up to 0.1 M) may be used to estimate sodium chloride activity coefficients. Following the additivity rule of Katchalsky et al.,[39] we do not include the fixed charges and their counterions in our calculation of the ionic strength inside the hydrogel. Our calculations show that the ratio of the mean ionic activity coefficient of sodium chloride in the hydrogel to that in the bath is always very close to unity; this fact may be behind the good agreement reported in the literature between experiment and swelling models employing ideal Donnan theory.[10,30]

A more advanced theory by Hasa et al.[51,61,65] is available for interpreting stress–strain measurements and swelling equilibria of polyelectrolyte networks. The theory of Hasa et al. takes into account the electrostatic repulsion of charges on the chains and also the finite extendibility (non-Gaussian behavior) of the chains. This theory contains a parameter *s*, the number of monomer units in a statistical segment, that is typically fit to data or determined from independent experiments. Using a reasonable value for *s* (4.0) for polyacrylamide networks, our calculations show that the electrostatic repulsion terms are negligible; the charge density of the hydrogels in this study is too low for fixed-charged repulsions to be significant. Aslo, as discussed above, we have chosen not to use non-Gaussian corrections in this study.

Kinetic models of network formation have been developed by Miller and Macosko[66–68] and by Tobita and Hamielec.[46,69] These models may be used to calculate average network properties such as the cross-link density and molecular weight between cross-links, provided that the reactivity ratios for the monomers are known. Tobita and Hamielec[69] have developed a kinetic model for the free-radical copolymerization of acrylamide and *N,N*′-methylenebis(acrylamide) (BIS). Confirming the results of various studies,[11,70–72] the model of Tobita and Hamielec predicts that inhomogeneous, imperfect networks are formed by copolymerizing acrylamide with BIS. We did not attempt to use the kinetic models mentioned above to predict network properties because reactivity ratios for the acrylamide–BIS–MAPTAC terpolymerization are not currently available.

Conclusions

Cationic acrylamide-based hydrogels were prepared with the same overall composition and with different initial total monomer concentrations % *T*. Hydrogel swelling equilibria in pure water were observed to decline dramatically with rising % *T*. Raising the % *T* in the pregel reaction mixture allows for increased chain interpenetration and improved efficiency of the cross-linking reaction in the resulting hydrogel.

Mechanical compressive stress–strain measurements were performed on % *T*-varying hydrogels equilibrated in pure water. The results are consistent with those expected for highly swollen networks; fair agreement is obtained with the phantom theory of elasticity.

The Donnan exclusion of sodium ions from the cationic hydrogels was measured in order to estimate the fixed-charge densities of the hydrogels. The results show one-third of the cationic charges apparently missing. It is postulated that some of the cationic charges were masked in the Donnan-exclusion experiments by anionic carboxylate functionalities placed on the network chains by the hydrolysis of pendant amide groups.

Good agreement between theory and experiment is obtained for % *T*-varying hydrogels equilibrated in aqueous NaCl. The good agreement is facilitated by fitting a parameter N in the swelling model to swelling equilibria for the hydrogels in deionized water. N is a weak function of $\%T$, is of order unity, and serves to correct for deficiencies in the theoretical description of hydrogel swelling.

Acknowledgment. This work was supported by the Director, Office of Energy Research, Office of Basic Energy Sciences, Chemical Sciences Division of the U.S. Department of Energy under Contract Number DE-AC03-76SF00098. Additional support was provided by the National Institutes of Health under Grant Number R01 GM46788-01. The authors are grateful to D. Devens for performing the compression–strain measurements and to A. P. Sassi, D. S. Soane, J. E. Mark, and R. A. Siegel for helpful discussions.

References and Notes

(1) Allen, R. C., Maurer, H. R., Eds. *Electrophoresis and Isoelectric Focusing in Polyacrylamide Gels*; de Gruyter: Berlin, 1974.
(2) Bio-Rad Laboratories *Bulletin 1156*: *Acrylamide Polymerization—A Practical Approach*, Bio-Rad Chemical Division: Richmond, CA, 1987.
(3) Chrambach, A.; Rodbard, D. *Science* **1971**, *172*, 440.
(4) Geissler, E.; Hecht, A.-M.; Horkay, F.; Zrinyi, M. *Macromolecules* **1988**, *21*, 2594.
(5) Hasa, J.; Janacek, J. *J. Polym. Sci.: Part C* **1967**, *16*, 317.
(6) Janacek, J.; Hasa, J. *Collect. Czech. Chem. Commun.* **1966**, *31*, 2186.
(7) Oppermann, W.; Rose, S.; Rehage, G. *Br. Polym. J.* **1985**, *17* (2), 175.
(8) Katayama, S.; Yamazaki, F.; Akahori, Y. *J. Phys. Chem.* **1993**, *97*, 290.
(9) Ilavsky, M.; Hrouz, J. *Polym. Bull.* **1983**, *9*, 159.
(10) Hooper, H. H.; Baker, J. P.; Blanch, H. W.; Prausnitz, J. M. *Macromolecules* **1990**, *23*, 1096.
(11) Rüchel, R.; Steere, R. L.; Erbe, E. F. *J. Chromatogr.* **1978**, *166*, 563.
(12) Flory, P. J.; Rehner, J., Jr. *J. Chem. Phys.* **1943**, *11* (11), 521.
(13) Flory, P. J. *Principles of Polymer Chemistry*; Cornell University Press: Ithaca, NY, 1953.
(14) Baker, J. P.; Blanch, H. W.; Prausnitz, J. M. LBL Report No. 33533, Lawrence Berkeley Laboratory: Berkeley, CA, 1993.
(15) Frenkel, J. *Rubber Chem. Technol.* **1940**, *13*, 264.
(16) Gee, G.; Herbert, J. B. M.; Roberts, R. C. *Polymer* **1965**, *6*, 541.
(17) Yen, L. Y.; Eichinger, B. E. *J. Polym. Sci., Polym. Phys. Ed.* **1978**, *16*, 121.
(18) Brotzman, R. W.; Eichinger, B. E. *Macromolecules* **1981**, *14*, 1445.
(19) Brotzman, R. W.; Eichinger, B. E. *Macromolecules* **1982**, *15*, 531.
(20) Brotzman, R. W., Jr.; Eichinger, B. E. *Macromolecules* **1983**, *16* (7), 1131.
(21) Neuburger, N. A.; Eichinger, B. E. *Macromolecules* **1988**, *21*, 3060.
(22) Deloche, B.; Samulski, E. T. *Macromolecules* **1988**, *21*, 3107.
(23) Zhao, Y.; Eichinger, B. E. *Macromolecules* **1992**, *25*, 6988.
(24) Zhao, Y.; Eichinger, B. E. *Macromolecules* **1992**, *25*, 6996.
(25) McKenna, G. B.; Flynn, K. M.; Chen, Y. *Macromolecules* **1989**, *22*, 4507.
(26) Horkay, F.; Hecht, A.-M.; Geissler, E. *Macromolecules* **1989**, *22*, 2007.
(27) Horkay, F.; Hecht, A. M.; Geissler, E. *J. Chem. Phys.* **1989**, *91* (4), 2706.
(28) Horkay, F.; Burchard, W.; Geissler, E.; Hecht, A.-M. *Macromolecules* **1993**, *26*, 1296.
(29) Geissler, E.; Horkay, F.; Hecht, A.-M. *Macromolecules* **1991**, *24*, 6006.
(30) Ricka, J.; Tanaka, T. *Macromolecules* **1984**, *17*, 2916.
(31) Prange, M.; Hooper, H. H.; Prausnitz, J. M. *AIChE J.* **1989**, *35*, 803.
(32) Marchetti, M.; Prager, S.; Cussler, E. L. *Macromolecules* **1990**, *23*, 1760.
(33) Oppermann, W. In *Polyelectrolyte Gels*; Harland, R. S., Prud'homme, R. K., Eds.; ACS Symposium Series 480; American Chemical Society: Washington, DC, 1992; pp 159–170.
(34) Harsh, D. C.; Gehrke, S. H. In *Absorbent Polymer Technology*; Brannon-Peppas, L., Harland, R. S., Eds.; Elsevier: Amsterdam, 1990; pp 103–124.
(35) James, H. M.; Guth, E. *J. Chem. Phys.* **1947**, *15*, (9), 669.
(36) Mark, J. E.; Erman, B. *Rubberlike Elasticity A Molecular Primer*; Wiley: New York, 1988.
(37) Ilavsky, M.; Dusek, K. *Polym. Bull.* **1979**, *1*, 801.
(38) Treloar, L. R. G. *The Physics of Rubber Elasticity*; University Press: Oxford, 1975.
(39) Katchalsky, A. *Pure Appl. Chem.* **1971**, *26*, 327.
(40) Pak, H.; Flory, P. J. *J. Polym. Sci., Polym. Phys. Ed.* **1979**, *17*, 1845.
(41) Erman, B.; Flory, P. J. *J. Polym. Sci., Polym. Phys. Ed.* **1978**, *16*, 1115.
(42) Mark, J. E. *Polym. Eng. Sci.* **1979**, *19* (4), 254.
(43) Mark, J. E. *Polym. Eng. Sci.* **1979**, *19* (6), 409.
(44) Overbeek, J. Th. G. *Prog. Biophys. Biophys. Chem.* **1956**, *6*, 58.
(45) Richards, E. G. *An Introduction to Physical Properties of Large Molecules in Solution*; Cambridge University Press: Cambridge, 1980.
(46) Tobita, H.; Hamielec, A. E. *Polymer* **1990**, *31*, 1546.
(47) Ball, R. C.; Doi, M.; Edwards, S. F.; Warner, M. *Polymer* **1981**, *22*, 1010.
(48) Edwards, S. F.; Vilgis, T. *Polymer* **1986**, *27*, 483.
(49) Peppas, N. A.; Merrill, E. W. *J. Appl. Polym. Sci.* **1977**, *21*, 1763.
(50) Hill, T. L. *An Introduction to Statistical Thermodynamics*; Addison-Wesley: Reading, MA, 1960.
(51) Hasa, J.; Ilavsky, M.; Dusek, K. *J. Polym. Sci., Polym. Phys. Ed.* **1975**, *13*, 253.
(52) Vasheghani-Farahani, E.; Vera, J. H.; Cooper, D. G.; Weber, M. E. *Ind. Eng. Chem. Res.* **1990**, *29*, 554.
(53) Kheradmand, H.; Francois, J.; Plazanet, V. *Polymer* **1988**, *29*, 860.
(54) Truong, N. D.; Galin, J. C.; Francois, J.; Pham, Q. T. *Polymer* **1986**, *27*, 459.
(55) Higuchi, M.; Senju, R. *Polym. J.* **1972**, *3* (3), 370.
(56) Aksberg, R.; Wagberg, L. *J. Appl. Polym. Sci.* **1989**, *38*, 297.
(57) Ilavsky, M.; Hrouz, J.; Stejskal, J.; Bouchal, K. *Macromolecules* **1984**, *17*, 2868.
(58) Streitwieser, A., Jr.; Heathcock, C. H. *Introduction to Organic Chemistry*, Macmillan: New York, 1981.
(59) Baker, J. P.; Stephens, D. R.; Blanch, H. W.; Prausnitz, J. M. *Macromolecules* **1992**, *25*, 1955.
(60) Katayama, S.; Myoga, A.; Akahori, Y. *J. Phys. Chem.* **1992**, *96*, 4698.
(61) Ilavsky, M. *Adv. Polym. Sci.* **1993**, *109*, 173.
(62) Nicoli, D.; Young, C.; Tanaka, T.; Pollak, A.; Whitesides, G. *Macromolecules* **1983**, *16*, 887.
(63) Siegel, R. A.; Cornejo-Bravo, J. M. In *Polyelectrolyte Gels*; Harland, R. S., Prud'homme, R. K., Eds.; ACS Symposium Series 480; American Chemical Society: Washington, DC, 1992; pp 131–145.
(64) McQuarrie, D. A. *Statistical Mechanics*; Harper and Row: New York, 1976.
(65) Ilavsky, M. *Polymer* **1981**, *22*, 1687.
(66) Miller, D. R.; Macosko, C. W. *Macromolecules* **1976**, *9* (2), 206.
(67) Macosko, C. W.; Miller, D. R. *Macromolecules* **1976**, *9* (2), 199.
(68) Miller, D. R.; Macosko, C. W. *J. Polym. Sci., Part B: Polym. Phys.* **1987**, *25*, 2441.
(69) Tobita, H.; Hamielec. A. E. *Macromolecules* **1989**, *22*, 3098.
(70) Weiss, N.; Van Vliet, T.; Silberberg, A. *J. Polym. Sci., Polym. Phys. Ed.* **1979**, *17*, 2229.
(71) Hecht, A.-M.; Duplessix, R.; Geissler, E. *Macromolecules* **1985**, *18*, 2167.
(72) Cohen, Y.; Ramon, O.; Kopelman, I. J.; Mizrahi, S. *J. Polym. Sci., Part B: Polym. Phys.* **1992**, *30*, 1055.